Enhancement of limit of detection by inducing coffee-ring effect in water quality monitoring microfluidic paper-based devices

Rajesh Ghosh, Vijay Vaishampayan, Arpita Mahapatra, Richa Malhotra, Sivasamy Balasubramanian, Ashish Kapoor*

Department of Chemical Engineering, SRM Institute of Science and Technology, Kattankulathur, Tamil Nadu 603203, India, email: ghoshrajesh1226@gmail.com (R. Ghosh), setivijay@gmail.com (V. Vaishampayan), arpi1996@gmail.com (A. Mahapatra), mricha79@yahoo.com (R. Malhotra), balasubramanian.s@ktr.srmuniv.ac.in (S. Balasubramanian), ashishkapoorsrm@gmail.com (A. Kapoor)

ABSTRACT

Supply of safe drinking water is a challenging task requiring not only the availability of suitable devices but also satisfactory monitoring methods to ensure that the contaminants are present well within safe limits. In this context, microfluidic devices have recently emerged as promising technologies for point-of-use screening of water samples. These devices allow for easy interpretation, rapid and cost-effective analysis. The analytical approach employed in these devices for the detection of various water contaminants have different limits of detection that are bound by the nature and stoichiometry of the underlying chemical reaction. These limitations need to be addressed to make these devices more applicable and relevant for field analysis. In this work, we report a simple and novel technique to enhance the limit of detection for determining iron content in contaminated water. We utilize the coffee-ring phenomenon induced by outward capillary flows and differential evaporation rates on paper-based microfluidic devices. On addition of coloring agent, the response is obtained as a brown ring, analogous to the coffee-ring stain. The color intensity and the width of the ring are proportional to the concentration of iron in the water sample. The proposed scheme allowed a five-fold improvement in the limit of detection compared to the unmodified detection tests. The phenomenon can be utilized to enhance the signal from other heavy metal tests as well to enhance the limit of detection and bring these devices into their relevant market for widespread adoption.

Keywords: Microfluidics; Paper-based; Water quality monitoring; Limit of detection; Iron; Coffee-ring effect; Portable sensors

1. Introduction

Water quality monitoring is essential to determine the suitability of water for consumption and other applications. Deployment of suitable water treatment strategies and evaluation of their effectiveness rests upon analytical determination of concerned contaminants. Current established techniques include atomic absorption spectrophotometry [1,2], ion chromatography [3,4], inductively coupled plasma-mass spectrometry [5,6], potentiometry [7,8], UV-Vis spectrophotometry [9], and fluorescence spectroscopy [10]. Even though these state-of-the-art methods are precise and accurate, most of them are time-consuming and expensive, and require special sample preparation procedures to be carried out by trained personnel. Furthermore, time delays caused due to transportation of samples from the site of testing to analytical laboratories can also deteriorate the sample condition and impact the results. In this regard, scientific community has realized the need for development of low-cost, portable and on-the-spot detection methods [11]. Microfluidics based lab-on-a-chip platforms offer a promising alternative to address several of the aforementioned challenges. Particularly, microfluidic paper-based analytical devices

*Corresponding author.

(μ-PADs) have been explored for development of sensors for heavy metals, pathogens, and toxins. The usage of paper as a substrate offers unique advantages in terms of being inexpensive, disposable, portable, and amenable to surface modification. The fabrication methods involved in making paper-based devices are simple and do not require access to sophisticated equipment. Colorimetric reactions can be readily combined with μ-PADs to obtain qualitative or quantitative detection of target analytes of interest [12].

However, microfluidic paper-based analytical devices have still not received widespread implementation compared to their sophisticated conventional counterparts due to certain limitations in capabilities. Many of the μ-PADs offer a higher limit of detection (LOD) compared to established methods [13]. Attempts have been made to improve the detection capabilities by use of nanoparticles, structural modifications, and image processing techniques [14–16].

In this work, we employ ubiquitous phenomenon of coffee-ring effect along with a colorimetric based detection scheme and evaluate its effectiveness in improving limit of detection of target analyte. When a liquid solution droplet evaporates, it leaves behind deposits of suspended particles along the perimeter in a ring-like pattern, like a coffee stain. This phenomenon of coffee-ring effect is ascertained to capillary flow toward the edges caused by differential evaporation rates across the liquid region [17]. The mechanism has been utilized for achieving biomolecular separation [18], creation of 3D patterns of micro and nanoparticle assembly [19] and signal amplification in biosensors [20]. We successfully demonstrate application of this phenomena to drive analyte molecules toward the edges of detection zone, thereby improving the colorimetric signal output and enhancing limit of detection. The width of the ring serves as an additional signal output for determining concentration of analyte. The feasibility of the proposed strategy is shown using iron based colorimetric assay. The approach precludes usage of any other additives such as nanoparticles, surface modification protocols, peripheral equipment or sophisticated signal amplification methods. The strategy can prove to be viable for development of portable on-the-spot detection platforms with enhanced capabilities.

2. Materials and methods

2.1. Reagents and materials

Whatman® qualitative filter paper, grade 1 was sourced from Biogene life sciences, Chennai, India as a paper substrate for all the experiments. Punching machine (Kangaro Industries, India) and ink were obtained from local commercial store. Ammonium thiocyanate (NH_4CNS) and ammonium ferric sulphate ($NH_4Fe(SO_4)_2 \cdot 12H_2O$) were purchased from Thermo Fisher Scientific India Pvt. Ltd., Mumbai, India. Hydrochloric acid (HCl) was purchased from RFCL Ltd., New Delhi, India. Sulphuric acid was procured from Avantor Performance Materials India Limited, Mumbai, India. All chemical reagents used in the study were of analytical grade and used as received without further purification. Preparation of all salt solutions and dilutions was performed using deionized water.

2.2. Fabrication of devices

Paper-based devices used in this study comprise of hydrophilic paper adhered on a suitable support. Fig. 1 illustrates the primary steps involved in the fabrication procedure. A sheet of Whatman filter paper was punched using a punching machine commonly available in office supplies. The punched paper discs were used as the test substrates. The diameter of paper discs was measured to be 6+/–0.03 mm using a digital vernier calliper. The paper disc was adhered on a double sided adhesive tape that served as a support as well as prevented any leakage underneath the substrate. Five paper discs were adhered in an equidistant manner on a 6 cm long tape. The assembly was stored in a dry and airtight container for further use.

2.3. Contact angle measurements

The water contact angle was measured for the paper substrate using the sessile drop technique with an in-house fabricated setup. A water drop of 1 μL volume was gently placed on the surface of paper using a micropipette. The shape of drop was examined using a digital imaging device positioned perpendicular to the water-paper interface. Also, the imaging was done from the top to capture the spreading behavior of drop.

2.4. Experimental procedure

Stock solution of 1000 ppm of ammonium ferric sulphate (AFS) was prepared using 2N sulfuric acid and deionized water. Different aliquots of standard solution were prepared having iron concentration between 0 and 500 ppm. The fabricated paper devices were tested for detection of iron in aqueous solutions using iron thiocyanate as the colorimetric receptor. 2 μL of the reagent solution was added to each paper disc and allowed to air dry for 5 min. Following this, 3 μL of the iron containing aqueous sample was added twice onto the chemically modified paper discs and the color formation was observed. The set up was left undisturbed for 1 min to allow for stabilization of the color. The colored paper disc was digitally photographed inside a light box. The sequence of addition of the sample and the reagent was investigated. While the addition of reagent as the first step in the sequence resulted in color formation on the entire disc, the vice versa sequence led to the induction of the coffee-ring effect near the periphery of paper disc. This phenomenon was utilized to concentrate the metallic ions at the periphery of the paper disc leading to strong colorimetric signal and enhanced limit of detection. For this, 3 μL of iron containing sample was added twice onto the paper discs followed by the addition of 2 μL of reagent solution. Sufficient time was allowed for drying of the paper discs after each volumetric addition and also to avoid flooding of the test region that could lead to erroneous results. Being only 6 mm in diameter, the paper discs could be loaded with a limited volume (6 μL) of sample or reagent at a time. The paper discs were covered with a non-porous opaque sheet if there was any delay in acquiring images after performing reactions. The experiments were conducted in triplicates to ensure repeatability.
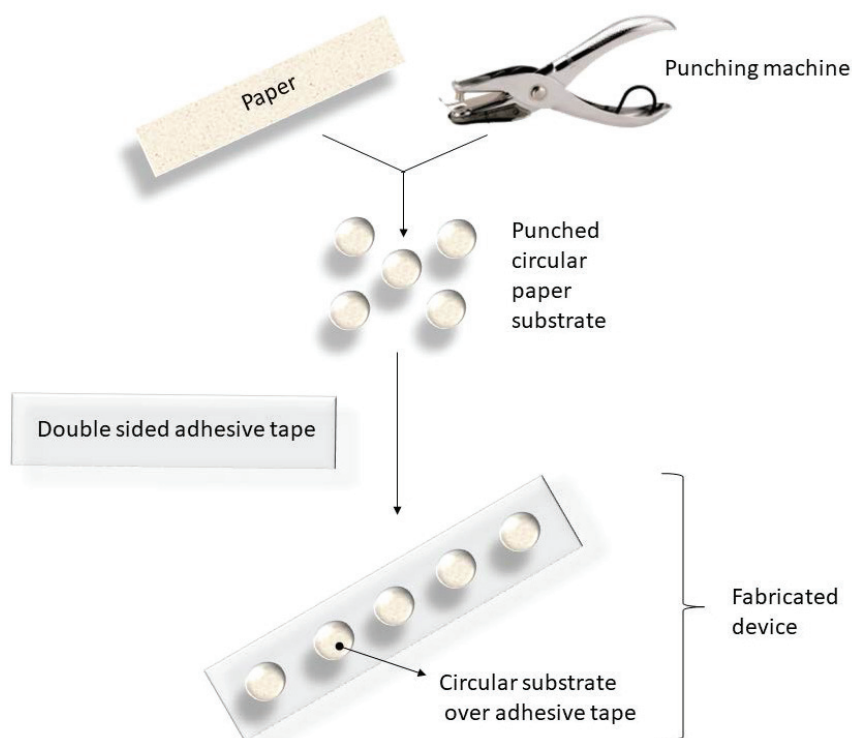
Fig. 1. Schematic illustration of steps involved in the fabrication of microfluidic paper-based device.

2.5. Image acquisition and analysis

The detection of iron involves color changes on paper discs that need to be analyzed for quantification of data. This was accomplished by acquiring digital images of the paper discs, and analyzing them with image processing software tools. All images were captured using a smartphone camera (Panasonic Eluga Note) at default camera settings without flash. The imaging samples were placed in an in-house fabricated light box with uniform lighting while capturing the images. The light box had dimensions of $10 \times 10 \times 10$ cm and was equipped with light-emitting diode (LED) lights amounting to 4000 lux lighting conditions. The images captured using the smartphone were transferred to a computer for further processing and interpretation. The image analysis procedure using Adobe Photoshop software is described here briefly. The circular hydrophilic detection zone, our region of interest was demarcated with the help of quick selection tool. The color average tool was employed to average the color in the entire selected region. Eyedropper tool was then used to obtain primary color component (red, green and blue (RGB)) intensities for the specific image. The procedure was repeated for all images and RGB values were recorded. Average greyscale intensity (I) was calculated using RGB intensity values using the following formula.

$$\text{Greyscale intensity I} = 0.2126R + 0.7152G + 0.0722B \qquad (1)$$

where R, G, and B correspond to red, green and blue color intensities respectively.

The values were subsequently inverted and compared for various detection experiments.

3. Results and discussion

3.1. Punched paper discs as detection devices

The paper-based detection devices used here comprised of hydrophilic filter paper discs of 6 mm diameter. Creating hydrophilic zones or channels confined by hydrophobic boundaries is one of the most popular techniques for paper based analytical devices [21]. However, it typically needs access to wax printing. Furthermore, wax impregnation through the paper needs to be optimized and such wax confined test zones and channels are not viable in presence of organic solvents surfactants that can dissolve wax [22]. An alternative approach of paper cutting has been adopted by researchers to fabricate paper-based devices of desired shapes and designs [23,24]. Our fabrication approach employs a simpler version of paper cutting by making use of commonly used punching machine. Unless very fine resolution features are required, using punched paper disc as detection zone for colorimetric reaction serves as a relatively more user-friendly, simpler and easier method for fabrication and testing. The punched paper can be easily supported on various types of substrates without any special bonding techniques. We used double-sided adhesive tape for holding the paper discs in fixed position. It allowed for easy handling while transport and storage.

3.2. Hydrophilicity

Hydrophilicity of the paper substrate is an important parameter for determining its viability as the detection zone in lab-on-a-chip devices. Contact angle measurement was

used to quantify the hydrophilic characteristics of paper substrate. The liquid drop used for measuring the contact angle completely spread out on the solid surface suggesting perfect wetting with contact angle nearly 0 degree. The behavior is depicted in schematic illustration (Fig. 2). The wettability was also visually confirmed by using a colored dye solution. When introduced at the center of the circular detection zone, the colored liquid was uniformly wicked in radially outward direction by capillary action.

3.3. Parameter optimization

The role of various experimental parameters and their possible interactions become important when working with minute amounts of reagents and samples in miniaturized devices [25]. The dimension of paper disc substrate used as the detection zone was kept fixed in all the experiments. Preliminary trials revealed a few factors that can affect the detection performance of the device. A brief summary of such factors is discussed here. The low volume of liquid used in the microfluidic devices is one of their attractive features. Hence it is important to optimize the volume such that the capability of device remains uncompromised. Excess volume could cause leakage or overflow from the paper disc, while too low volumes would not cover the detection zone completely hence affecting the performance. Hence volume must be appropriately selected as per the dimensions of detection zone. In our experiments, 2 µL was the minimum volume required to cover the complete detection zone and approximately 6 µL was the maximum volume that could be used without any overflow of liquid.

Furthermore, the volume ratios of reagent and sample used for colorimetric reaction are also important to achieve the best readout signal. It is necessary to maintain an appropriate ratio that would aid in achieving products with uniform and intense color in detection zone even at lower range of concentration. The optimal volume ratio for volume of reagent to that of analyte containing sample for our experiments was observed to be 1:3. Lighting conditions have been reported to affect the signal readout and interpretation of results in portable microfluidic detection platforms [26]. To avoid any bias due to lighting, all images were acquired using an indigenous light box that maintained intensity around 4000 lux. The intensity was measured periodically to ensure stability of light conditions.

3.4. Iron detection

The formation of colored complex Fe(III)-ammonium thiocyanate formed the basis of detection of iron. Fig. 3 shows the experimental observations for various concentrations of iron in water. The color in detection zone became more intense as iron concentration was increased. The data was used for quantification of iron concentration and generation of calibration chart for estimation of iron. The colour intensity was obtained from RGB analysis of each colored image. The calibration chart is plotted for iron concentration in sample ranging from 0 to 500 ppm as shown in Fig. 4. The error bars indicate standard deviations (SD) for multiple experimental data points. The data is fitted and $y = 70.807x^{0.1978}$ is found to be the best fit with coefficient

Fig. 2. Schematic representation of complete wetting on paper substrate.

Fig. 3. Effect of change in concentration of iron on the color intensity. All the concentration values (ppm) are indicated in the center of digital image of each paper disc. Blank corresponds to zero ppm iron solution.
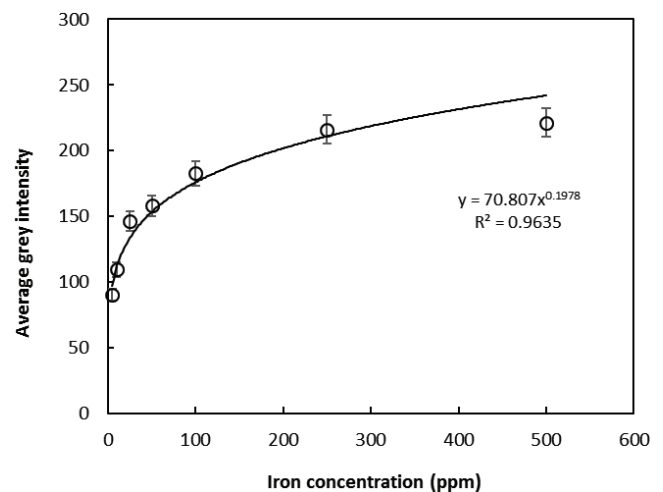
Fig. 4. Calibration curve for average grey intensity versus iron concentration. The values represent mean ± standard deviation (SD) of triplicates.

of determination R^2 of 0.9635, where y and x represent the average grey intensity and the concentration of iron, respectively. The non-linear trend of calibration plot is in agreement with observations reported for colorimetric assays on paper-based platforms. The observed behavior is attributed to the fact that with the increase in analyte concentration, the surface of detection zone becomes saturated resulting in flattening of the plot at higher concentrations.

Estimation of iron is of practical interest due to its role in chemical and biological processes. Even though iron intake is crucial for human beings due to its involvement in hemoglobin synthesis, a chronic consumption of iron overdose can pose health problems. Iron occurs naturally in groundwater in small proportions, but its concentration

is increased in certain regions due to various natural and anthropogenic factors including leaching of iron salts from rocks, corrosion of pipes, and release from solid wastes [27]. The well-established methods of iron estimation involve use of sophisticated equipment. However, in order to make analysis accessible for common populace living in regions of concern, it is essential to have on-the-spot tests to quickly estimate iron content in water and ensure its viability for consumption. Asano et al. have demonstrated a paper-based device for iron assay using iron-phenanthroline chemistry [28]. Although the devices fabricated by their approach had high resolution and stability, the fabrication procedure involved photolithographic technique that is expensive, largely inaccessible and needs trained professionals for operation. The fabrication method and detection procedure used here can be easily adopted with minimal resource availability.

3.5. Coffee-ring effect analysis

The modified experimental procedure induced accumulation of iron species in peripheral region that resulted in colored ring formation by Fe-thiocyanate colorimetric reaction. The digital image data collected for various concentration of iron with induced coffee-ring effect is shown in Fig. 5. The color tone varied with increment in iron concentration. The sample for 500 ppm iron concentration was not included in this analysis as the major portion of paper disc was saturated with high intensity color complex and coffee-ring was not visually prominent. The water sample with 1 ppm iron concentration also exhibited a thin brown ring near the periphery. This was a five-fold improvement in limit of detection compared to unmodified procedure (5 ppm).

The mechanism of coffee-ring effect (Fig. 6) can be explained as follows. The rate of evaporation is highest at the edges. As the liquid evaporates, it induces capillary flow from the center toward the edges to replenish the evaporating liquid. It brings along the suspended particles (here iron) toward the edges. Once a colored complex is formed by reaction between reactants, relatively higher color intensification is observed in the peripheral region in comparison to that at the central region.

In order to quantify the data obtained from images, three methods of image analyses were investigated. In the first method, color was averaged over the entire detection zone as done for the unmodified experimental data and subsequently used for RGB intensity analysis. The calibration chart for iron using the first method is illustrated in Fig. 7a. The calibration curve followed a non-linear equation $y = 125.09x^{0.0873}$ with a coefficient of determination of 0.9485, where y and x represent the average grey intensity and the concentration of iron, respectively. Our experimental results indicated that width of the colored ring also varied with concentration of iron. The second method employed color averaging only in the respective ring widths for each image. The approach helped in eliminating white or less intense color from being used in averaging and intensity calculations. The calibration curve (Fig. 7b) generated by this method followed the equation $y = 145.87x^{0.0678}$ with R^2 value of 0.9738, where y and x represent the average grey intensity and the concentration of iron, respectively. The
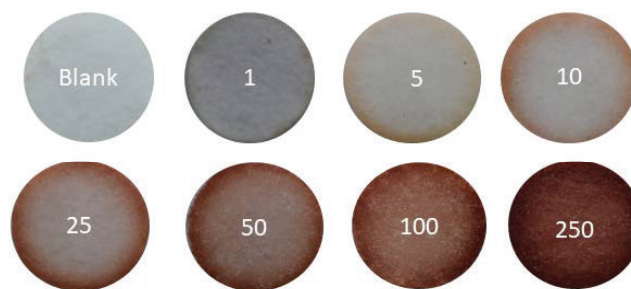
Fig. 5. Effect of change in concentration of iron on the color intensity with coffee-ring effect. All the concentration values (ppm) are indicated in the center of digital image of each paper disc. Blank corresponds to zero ppm iron solution.
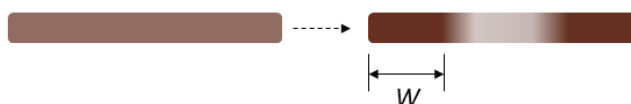
Fig. 6. Schematic representation of color intensification due to coffee-ring effect. W – represents the width of the ring.

third approach of image analysis employed dimensional measurements instead of intensity calculations as adopted by other researchers for immunoassay quantification [17]. In this case, width of ring was directly correlated to corresponding iron concentration. The calibration curve (Fig. 7c) obtained using the dimensional measurement approach also fits the data well in a non-linear expression $y = 0.0737x^{0.4276}$ with $R^2 = 0.9622$, where y and x represent the width of the ring and the concentration of iron, respectively. The goodness of fit indicates that either of the above mentioned three approaches could be used for the estimation of concentration of iron.

Our method offers two simultaneous visual signals that can be used to quantify concentration of unknown species in sample. Firstly, the formation of colored iron thiocyanate complex gives a visible colorimetric signal. The color intensity varies as a function of Fe concentration in the sample as shown in the calibration charts (Figs. 7a,b) that can be used for analysis by image processing and intensity calculations. Additionally, the colored complex forms a ring of specific width for a fixed concentration. As observed in Fig. 5, coffee-ring type patterns of different widths are formed for different iron concentration and corresponding calibration curve shown in Fig. 7c can used for quantitative analysis.

The coffee-ring pattern width can be a function of several parameters including liquid drop volume, contact angle, humidity and concentration. In all experiments, same paper substrate was used and liquid droplets were primarily aqueous. Thus the contact angle remained fixed for liquid-solid interface. Under constant humidity conditions and fixed liquid volumes, coffee-ring pattern width was primarily a function of concentration of iron species in the sample. The selection of paper as a substrate offers unique benefits for performing coffee-ring effect-based experiments. Earlier research has shown that porous substrates are preferred to smooth planar solid substrates for quantification of signal obtained from coffee ring effect [18].

(a)

(b)

(c)
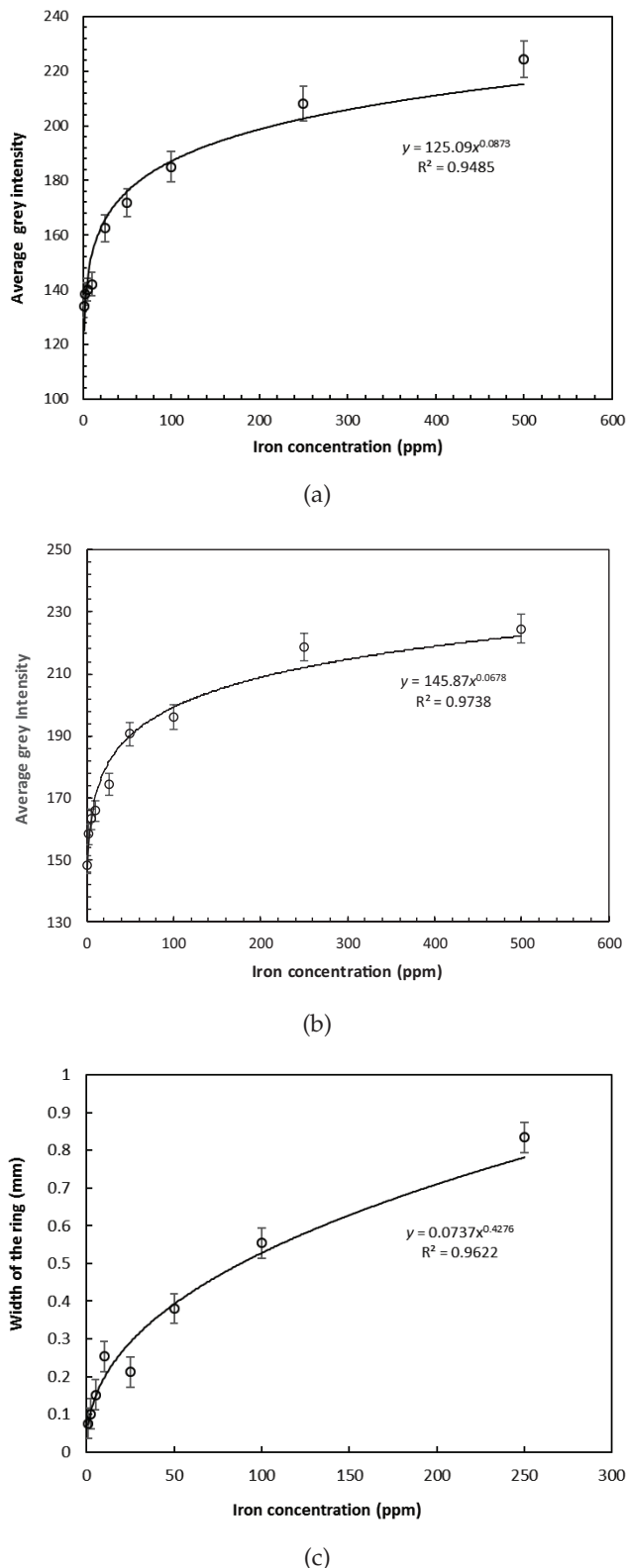
Fig. 7. a,b Calibration curve for average grey intensity versus iron concentration with coffee-ring effect. Where, (a) corresponds to color averaging done over entire paper disc and (b) corresponds to color averaging done over the width of the ring. (c) is the calibration curve for width of the ring versus iron concentration. The values represent mean ± standard deviation (SD) of triplicates.

The unrestricted motion of solid particles towards the edges of evaporating liquid on smooth surfaces is hindered due to porous matrix in paper. As the particles get adsorbed in the matrix during their edgeward motion, the ring is no longer restricted to the periphery. It expands radially inward making the quantification easier. The increasing width of coffee-ring pattern with increase in concentration of iron in liquid samples (Fig. 5) agree with the similar phenomena observed for enzyme-linked immunosorbent assays [18]. Dual signal output from same experiment allows the user to select the appropriate method depending on one's accessibility to imaging and image processing facilities.

A qualitative point-of-use detection assay requires naked eye visualization for a "yes" or "no" answer to infer presence or absence of contaminant of concern. However, a quantitative assay requires image acquisition, processing, analysis and interpretation of data by comparing to a calibration chart. The assay demonstrated here can be utilized for either of the types of detection as per resource availability and requirements. It must be noted that the qualitative application is limited to visual interpretation of results. The development of color or lack of it on bringing together sample and reagent serves as a rapid and on-the-spot naked eye readout for identification of iron in water sample. Both qualitative and quantitative analyses would benefit from improving the limit of detection.

4. Conclusion

We have presented a simple strategy to enhance the limit of detection in microfluidic paper-based analytical devices and demonstrated it for estimation of iron contamination in water. The mechanism is based on the differential evaporation phenomenon on the surface of the paper that induces coffee-ring pattern formation on the substrate and amplifies the colorimetric signal. It is clear from the study that two forms of optical signals on the substrate, namely color intensity and width of the colored ring are obtained as a function of analyte concentration. The visual data can be readily used for qualitative and/or quantitative interpretation of results using minimal or no specialized data analysis resources. The approach demonstrated here is likely to propel development of portable and low-cost environmental monitoring platforms with improved capabilities for applications in resource limited settings.

References

[1] S.D. Richardson, A.T. Thomas, Water analysis: emerging contaminants and current issues, Anal. Chem., 90(1) (2018) 398–428.

[2] N. Rahmanian, S.H.B. Ali, M. Homayoonfard, N.J. Ali, M. Rahan, A.S. Nizami, Analysis of physiochemical parameters to evaluate the drinking water quality in the State of Perak, Malaysia, J. Chem., 8 (2015) 1–10.

[3] K. Brindha, R. Rajesh, R. Murugan, L. Elango, Fluoride contamination in groundwater in parts of Nalgonda District, Andhra Pradesh, India, Environ. Monit. Assess., 172(1–4) (2011) 481–492.

[4] M.A. Seiler, D. Jensen, U. Neist, U.K. Deister, F. Schmitz, Validation data for the determination of perchlorate in water using ion chromatography with suppressed conductivity detection, Environ. Sci. Eur., 28(1) (2016) 1–9.

[5] R.M. Abdul, L. Mutnuri, P.J. Dattatreya, D.A. Mohan, Assessment of drinking water quality using ICP-MS and microbiological methods in the Bholakpur area, Hyderabad, India, Environ. Monit. Assess., 184(3) (2012) 1581–1592.

[6] M.S. Islam, M.K. Ahmed, M. Raknuzzaman, M. Habubullah-Al-Mamun, M.K. Islam, Heavy metal pollution in surface water and sediment: a preliminary assessment of an urban river in a developing country, Ecol. Indic., 48 (2015) 282–291.

[7] A. Ceresa, E. Bakker, B. Hattendorf, D. Günther, E. Pretsch, Potentiometric polymeric membrane electrodes for measurement of environmental samples at trace levels: New requirements for selectivities and measuring protocols, and comparison with ICPMS, Anal. Chem., 73(2) (2001) 343–351.

[8] A. Nemiroski, D.C. Christodouleas, J.W. Hennek, A.A., E.J. Maxwell, G.M. Whitesides, Universal mobile electrochemical detector designed for use in resource-limited applications, Proc. Natl. Acad. Sci. USA, 111(33) (2014) 11984–11989.

[9] M.S. Noorashikin, A.B. Nur Nadiah, I. Nurain, A.A. Siti Aisyah, M.R. Siti Zulaika, Determination of phenol in water samples using cloud point extraction and UV spectrophotometry, Desal. Water Treat., 57(33) (2016) 15486–15494.

[10] M. Heibati, C.A. Stedmon, K. Stenroth, S. Rauch, J. Toljander, M. Säve-Söderbergh, K.R. Murphy, Assessment of drinking water quality at the tap using fluorescence spectroscopy, Water Res., 125 (2017) 1–10.

[11] A. Gałuszka, Z.M. MIgaszewski, J. Namieśnik, Moving your laboratories to the field–advantages and limitations of the use of field portable instruments in environmental sample analysis, Environ. Res., 140 (2015) 593–603.

[12] C. Dincer, R. Bruch, A. Kling, P.S. Dittrich, G.A. Urban, Multiplexed point-of-care testing–xPOCT, Trends Biotechnol., 35(8) (2017) 728–742.

[13] M. Sher, R. Zhuang, U. Demirci, W. Asghar, Paper-based analytical devices for clinical diagnosis: recent advances in the fabrication techniques and sensing mechanisms, Expert Rev. Mol. Diagn., 17(4) (2017) 351–366.

[14] E.M. Linares, L.T. Kubota, J. Michaelis, S. Thalhammer, Enhancement of the detection limit for lateral flow immunoassays: evaluation and comparison of bioconjugates, J. Immunol. Methods, 375(1–2) (2012) 264–270.

[15] L. Rivas, M. Dedina-Sánchez, A. de la Escosura-Muñiz, A. Merkoçi, Improving sensitivity of gold nanoparticle-based lateral flow assays by using wax-printed pillars as delay barriers of microfluidics, Lab Chip, 14(22) (2014) 4406–4414.

[16] K.E. McCracken, S.V. Angus, K.A. Reynolds, J.Y. Yoom, Multimodal imaging and lighting bias correction for improved µPAD-based water quality monitoring via smartphones, Sci. Rep., 6 (2016) 27529.

[17] D. Zhang, B. Gao, Y. Chen, H. Liu, Converting colour to length based on the coffee-ring effect for quantitative immunoassays using a ruler as readout, Lab Chip, 18(2) (2018) 271–275.

[18] T.S. Wong, T.H. Chen, X. Shen, C.M. Ho, Nanochromatography driven by the coffee ring effect, Anal. Chem., 83(6) (2011) 1871–1873.

[19] S. Choi, S. Stassi, A.P. Pisano, T.I. Zohdi, Coffee-ring effect-based three dimensional patterning of micro/nanoparticle assembly with a single droplet. Langmuir, 26(14) (2010) 11690–11698.

[20] J.T. Wen, C.M. Ho, P.B. Lillehoj, Coffee ring aptasensor for rapid protein detection, Langmuir, 29(26) (2013) 8440–8446.

[21] D.D. Liana, B. Raguse, J.J. Gooding, E. Chow, Recent advances in paper-based sensors, Sensors, 12(9) (2012) 11505–11526.

[22] J.H. Shin, J. Park, J.K. Park, Organic solvent and surfactant resistant paper-fluidic devices fabricated by one-step embossing of nonwoven polypropylene sheet, Micromachines, 8(1) (2017) 30.

[23] P. Kauffman, E. Fu, B. Lutz, P. Yager, Visualization and measurement of flow in two-dimensional paper networks, Lab Chip, 10(19) (2010), 2614–2617.

[24] W. Wang, W.Y. Wu, J.J. Zhu, Tree-shaped paper strip for semiquantitative colorimetric detection of protein with self-calibration, J. Chromatogr. A, 1217(24) (2010) 3896–3899.

[25] B.M. Jayawardane, S. Wei, I.D. McKelvie, S.D. Kolev, Microfluidic paper-based analytical device for the determination of nitrite and nitrate, Anal. Chem., 86(15) (2014) 7274–7279.

[26] D.M. Cate, J.A. Adkins, J. Mettakoonpitak, C.S. Henry, Recent developments in paper-based microfluidic devices, Anal. Chem., 87(1) (2015) 19–41.

[27] K.K. Borah, B. Bhuyan, H.P. Sarma, Lead, arsenic, fluoride, and iron contamination of drinking water in the tea garden belt of Darrang district, Assam, India, Environ. Monit. Assess., 169(1–4) (2010) 347–352.

[28] H. Asano, Y. Shiraishi, Development of paper-based microfluidic analytical device for iron assay using photomask printed with 3D printer for fabrication of hydrophilic and hydrophobic zones on paper by photolithography, Anal. Chim. Acta, 883(2015) 55–60.